THE QUASI-MOLECULAR STAGE OF TERNARY FISSION

D. N. POENARU AND B. DOBRESCU

Horia Hulubei National Institute of Physics and Nuclear Engineering,
P.O. Box MG-6, RO-76900 Bucharest, Romania
E-mail: poenaru@ifin.nipne.ro

W. GREINER

Institut für Theoretische Physik der Universität, Postfach 111932,
D-60054 Frankfurt am Main, Germany

J. H. HAMILTON AND A. V. RAMAYYA

Department of Physics, Vanderbilt University, Nashville, Tennessee, USA

We developed a three-center phenomenological model, able to explain qualitatively the recently obtained experimental results concerning the quasimolecular stage of a light-particle accompanied fission process. It was derived from the liquid drop model under the assumption that the aligned configuration, with the emitted particle between the light and heavy fragment, is reached by increasing continuously the separation distance, while the radii of the heavy fragment and of the light particle are kept constant. In such a way, a new minimum of a short-lived molecular state appears in the deformation energy at a separation distance very close to the touching point. This minimum allows the existence of a short-lived quasi-molecular state, decaying into the three final fragments. The influence of the shell effects is discussed. The half-lives of some quasimolecular states which could be formed in the ^{10}Be and ^{12}C accompanied fission of ^{252}Cf are roughly estimated to be the order of 1 ns, and 1 ms, respectively.

1 Introduction

The light particle accompanied fission was discovered [1] in 1946, when the track of a long-range particle (identified by Farwell *et al.* to be ^{4}He) almost perpendicular to the short tracks of heavy and light fragments was observed in a photographic plate. The fission was induced by bombarding ^{235}U with slow neutrons from a Be target at a cyclotron. The largest yield in such a rare process (less than one event per 500 binary splittings) is measured for α-particles, but many other light nuclei (from protons to oxygen or even calcium isotopes) have been identified [2] in both induced- and spontaneous fission phenomena. If A_1 and A_2 are the mass numbers of the heavy fragments (assume $A_1 \geq A_2$), then usually the mass of the light particle $A_3 << A_2$. The "true" ternary fission, in which $A_1 \simeq A_2 \simeq A_3$, has not yet been experimentally detected.

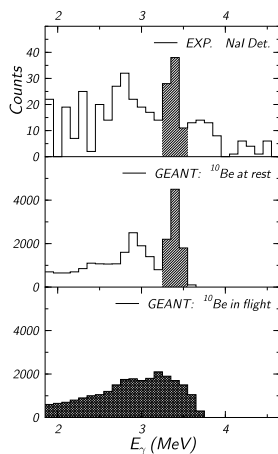Many properties of the binary fission process have been explained [3] within

Figure 1. Gamma-ray energy spectrum of ^{10}Be accompanying fission of ^{252}Cf (top) and the simulated (with the code GEANT) pulse-height distributions for a (not-Doppler-broadened) 3.37 MeV γ emission from ^{10}Be at rest (middle) as well as for ^{10}Be in flight (bottom) from the source to the detector (duration of about 1 ns). The flight-path of the order of 10 cm. One uses NaI scintillator detectors. Data from Fig. 6 of Ref. 13.

the liquid drop model (LDM); others like the asymmetric mass distribution of fragments and the ground state deformations of many nuclei, could be understood only after adding the contribution of shell effects. [4,5] As it was repeatedly stressed (see [6] and the references therein), shell effects proved also to be of vital importance for cluster radioactivities predicted [7] in 1980.

The total kinetic energy (TKE) of the fragments, in the most frequently detected binary or ternary fission mechanism, is smaller than the released energy (Q) by about 25–35 MeV, which is used to produce deformed and excited fragments. These then emitt neutrons (each with a binding energy of about 6 MeV) and γ-rays. From time to time a "cold" fission mechanism is detected, in which the TKE exhausts the Q-value, hence no neutrons are emitted, and the fragments are produced in or near their ground-state. The first experimental evidence for cold binary fission in which its TKE exhaust Q was reported [8] in 1981. Larger yields were measured [9] in trans-Fm ($Z \geq 100$) isotopes, where the phenomenon was called bimodal fission.

The correlated fragment pairs in cold ternary (α- and ^{10}Be accompanied spontaneous fission of ^{252}Cf) processes were only recently discovered, [10,11] by measuring triple γ coincidences in a modern large array of γ-ray detec-
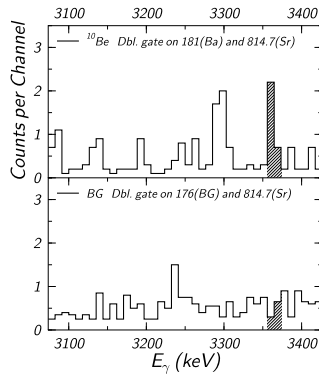
Figure 2. The cumulated γ-ray energy spectrum of ^{10}Be accompanying fission of ^{252}Cf (top) and the corresponding background (bottom). The spectrum of the 3.362 γ is not-Doppler-broadened, suggesting an emission from ^{10}Be at rest. The stopping time of ^{10}Be in the absorber mounted around the source is of the order of 1 ps. Data from Fig. 2 of Ref. 11. Coincidence spectra obtained with Ge detectors in GAMMASPHERE.

tors (GAMMASPHERE). The fragments are identified by their γ-ray spectra. Among other new aspects of the fission process seen for the first time with this new technique, [10,12] one should mention the double fine structure, and the triple fine structure in binary and ternary fission.

A particularly interesting feature, observed [11,13] both in ^{10}Be- and ^{12}C accompanied cold fission of ^{252}Cf is related to the width of the light particle γ-ray spectrum (see Figs. 1 and 2). For example, the 3.368 MeV γ line of ^{10}Be, with a lifetime of 125 fs is not Doppler-broadened, as it should be if it would be emitted when ^{10}Be is in flight (taking about 1 ns to reach the detector). A plausible suggestion was made, that the absence of Doppler broadening is related to a trapping of ^{10}Be in a potential well of nuclear molecular character. [11]

Quasi-molecular configurations of two nuclei have been suggested as a natural explanation for the resonances measured [14] in ^{12}C+^{12}C scattering and reactions. There are also other kinds of such binary molecules (see [15] and references therein), like spontaneously fissioning shape-isomers. The above mentioned experiments can be considered as the first evidence for a more complex quasi-molecular configuration of three nuclei. The purpose of the present lecture is to show, within a phenomenological three-center model, that a minimum which could explain the existence of these quasi-molecules is produced in the potential barrier, when the formation of the light particle

occurs in the neck between the two heavier fragments. In this way we extend to ternary fission our unified approach of cold fission, cluster radioactivities, and α-decay. [6]

2 Shape Parametrization

The shape parametrization with one deformation parameter as follows has been suggested from the analysis [16] of different aligned and compact configurations of fragments in touch. A lower potential barrier for the aligned cylindrically-symmetric shapes with the light particle between the two heavy fragments, is a clear indication that during the deformation from an initial parent nucleus to three final nuclei, one should arrive at such a scission point. In order to reach this stage we shall increase continuously the separation distance, R, between the heavy fragments, while the radii of the heavy fragment and of the light particle are kept constant, $R_1 = $ constant, $R_3 = $ constant. Unlike in the previous work, we now adopt the following convention: $A_1 \geq A_2 \geq A_3$. The hadron numbers are conserved: $A_1 + A_2 + A_3 = A$.

At the beginning (the neck radius $\rho_{neck} \geq R_3$) one has a two-center evolution (see Fig. 3) until the neck between the fragments becomes equal to the radius of the emitted particle, $\rho_{neck} = \rho(z_{s1}) \mid_{R=R_{ov3}} = R_3$. This Eq. defines R_{ov3} as the separation distance at which the neck radius is equal to R_3. By placing the origin in the center of the large sphere, the surface equation in cylindrical coordinates is given by:

$$\rho_s^2 = \begin{cases} R_1^2 - z^2 & , \quad -R_1 \leq z \leq z_{s1} \\ R_2^2 - (z-R)^2 & , \quad z_{s1} \leq z \leq R + R_2 \end{cases} \tag{1}$$
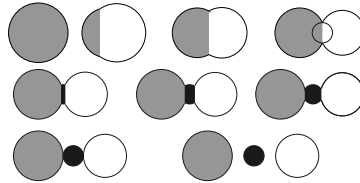

Figure 3. Evolution of nuclear shapes during the deformation process from one parent nucleus ^{252}Cf to three separated fragments ^{146}Ba, ^{10}Be, and ^{96}Sr. In the upper part the binary stage is illustrated; the separation distance increases from R_i to R_{ov3}, passing through R_{min1b} and R_{min2b} values. In the middle, the ternary stage of the process develops by forming the third particle in the neck. The quasi-molecular shape, at which $R = R_{min-t}$ is the intermediate one in this row. At the bottom the fragments are separated.

Then for $R > R_{ov3}$ the three center starts developing by decreasing progressively with the same amount the two tip distances $h_1 + h_{31} = h_{32} + h_2$. Besides this constraint, one has as in the binary stage, volume conservation and matching conditions. The R_2 and the other geometrical quantities are determined by solving numerically the corresponding system of algebraic equations. By assuming spherical nuclei, the radii are given by $R_j = 1.2249 A_j^{1/3}$ fm $(j = 0, 1, 3)$, $R_{2f} = 1.2249 A_2^{1/3}$ with a radius constant $r_0 = 1.2249$ fm, from Myers-Swiatecki's variant of LDM. Now the surface equation can be written as

$$\rho_s^2 = \begin{cases} R_1^2 - z^2 & , \quad -R_1 \leq z \leq z_{s1} \\ R_3^2 - (z - z_3)^2 & , \quad z_{s1} \leq z \leq z_{s2} \\ R_2^2 - (z - R)^2 & , \quad z_{s2} \leq z \leq R + R_2 \end{cases} \tag{2}$$

and the corresponding shape has two necks and two separating planes. Some of the important values of the deformation parameter R are the initial distance $R_i = R_0 - R_1$, and the touching-point one, $R_t = R_1 + 2R_3 + R_{2f}$. There is also R_{ov3}, defined above, which allows one to distinguish between the binary and ternary stage.

3 Deformation Energy

According to the LDM, by requesting zero energy for a spherical shape, the deformation energy, $E^u(R) - E^0$, is expressed as a sum of the surface and Coulomb terms

$$E_{def}^u(R) = E_s^0[B_s(R) - 1] + E_C^0[B_C(R) - 1] \tag{3}$$

where the exponent ^{u} stands for uniform (fragments with the same charge density as the parent nucleus), and ^{0} refers to the initial spherical parent. In order to simplify the calculations, we initially assume the same charge density $\rho_{1e} = \rho_{2e} = \rho_{3e} = \rho_{0e}$, and at the end we add the corresponding corrections. In this way we perform one numerical quadrature instead of six. For a spherical shape $E_s^0 = a_s(1 - \kappa I^2)A^{2/3}$; $I = (N - Z)/A$; $E_C^0 = a_c Z^2 A^{-1/3}$, where the numerical constants of the LDM are: $a_s = 17.9439$ MeV, $\kappa = 1.7826$, $a_c = 3e^2/(5r_0)$, $e^2 = 1.44$ MeV·fm.

The shape-dependent, dimensionless surface term is proportional to the surface area:

$$B_s = \frac{E_s}{E_s^0} = \frac{d^2}{2} \int_{-1}^{+1} \left[y^2 + \frac{1}{4}\left(\frac{dy^2}{dx}\right)^2 \right]^{1/2} dx \tag{4}$$
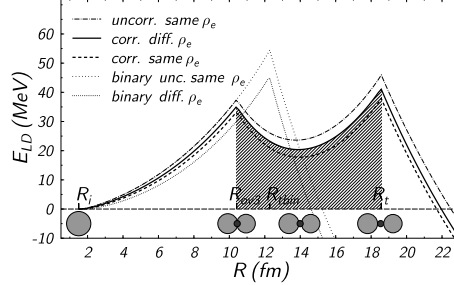
Figure 4. The liquid drop model deformation energy versus separation distance for the ^{20}O accompanied cold fission of ^{252}Cf with ^{132}Sn and ^{100}Zr heavy fragments. In order to simplify the numerical calculations we start by assuming the same charge density of the fragments. One can see the effect of successive corrections taking into account the experimental Q-value and the difference in charge density. Similar curves for the binary fission posses a narrower fission barrier. The new minimum appears in the shaded area from R_{ov3} to R_t.

where $y = y(x)$ is the surface equation in cylindrical coordinates with -1, +1 intercepts on the symmetry axis, and $d = (z'' - z')/2R_0$ is the seminuclear length in units of R_0. Similarly, for the Coulomb energy [17] one has

$$B_c = \frac{5d^5}{8\pi} \int\limits_{-1}^{+1} dx \int\limits_{-1}^{+1} dx' F(x, x') \tag{5}$$

$$
\begin{aligned}
F(x, x') = \{ & yy_1[(K - 2D)/3] \cdot \\
& \left[2(y^2 + y_1^2) - (x - x')^2 + \frac{3}{2}(x - x') \left(\frac{dy_1^2}{dx'} - \frac{dy^2}{dx} \right) \right] + \\
& K \left\{ y^2 y_1^2/3 + \left[y^2 - \frac{x - x'}{2} \frac{dy^2}{dx} \right] \left[y_1^2 - \frac{x - x'}{2} \frac{dy_1^2}{dx'} \right] \right\} \} a_\rho^{-1}
\end{aligned}
\tag{6}
$$

K, K' are the complete elliptic integrals of the 1st and 2nd kind

$$K(k) = \int\limits_0^{\pi/2} (1 - k^2 \sin^2 t)^{-1/2} dt; \quad K'(k) = \int\limits_0^{\pi/2} (1 - k^2 \sin^2 t)^{1/2} dt \tag{7}$$

and $a_\rho^2 = (y + y_1)^2 + (x - x')^2$, $k^2 = 4yy_1/a_\rho^2$, $D = (K - K')/k^2$.

The new minimum, which can be seen in Fig. 4 at a separation distance $R = R_{min-t} > R_{ov3}$, is the result of a competition between the Coulomb-

and surface energies. At the beginning ($R < R_{min-t}$) the Coulomb term is stronger, leading to a decrease in energy, but later on ($R > R_{min-t}$) the light particle formed in the neck posses a surface area increasing rapidly, so there is also an increase in energy up to $R = R_t$.

Now let us analyse the influence of various corrections, which could in principle alter this image. After performing numerically the integrations, we add the following corrections: for the difference in charge densities reproducing the touching point values; for experimental masses reproducing the Q_{exp}-value at $R = R_i$, when the origin of energy corresponds to infinite separation distances between fragments, and the phenomenological shell corrections δE

$$E_{LD}(R) = E_{def}^u(R) + (Q_{th} - Q_{exp})f_c(R) \tag{8}$$

where $f_c(R) = (R - R_i)/(R_t - R_i)$, and

$$Q_{th} = E_s^0 + E_C^0 - \sum_1^3 (E_{si}^0 + E_{Ci}^0) + \delta E^0 - \sum_1^3 \delta E^i \tag{9}$$

The correction increases gradually (see Fig. 4 and Fig. 5) with R up to R_t and then remains constant for $R > R_t$. The barrier height increases if $Q_{exp} < Q_{th}$ and decreases if $Q_{exp} > Q_{th}$. In this way, when one, two, or all final nuclei have magic numbers of nucleons, Q_{exp} is large and the fission barrier has a lower height, leading to an increased yield. In a binary decay mode like cluster radioactivity and cold fission, this condition is fulfilled when the daughter nucleus is ^{208}Pb and ^{132}Sn, respectively.

4 Shell Corrections and Half-lives

Finally we also add the shell terms

$$E(R) = E_{LD}(R) + \delta E(R) - \delta E^0 \tag{10}$$

Presently there is not available any microscopic three-center shell model reliably working for a long range of mass asymmetries. This is why we use a phenomenological model, instead of the Strutinsky's method, to calculate the shell corrections. The model is adapted after Myers and Swiatecki. [5] At a given R, we calculate the volumes of fragments and the corresponding numbers of nucleons $Z_i(R)$, $N_i(R)$ ($i = 1, 2, 3$), proportional to the volume of each fragment. Fig. 3 illustrates the evolution of shapes and of the fragment volumes. Then we add for each fragment the contribution of protons and neutrons

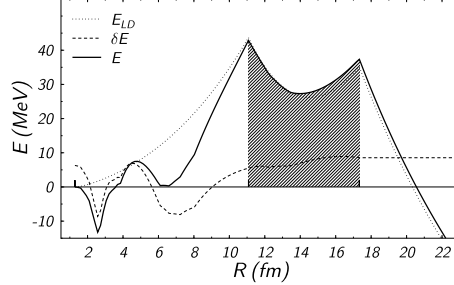$$\delta E(R) = \sum_i \delta E_i(R) = \sum_i [\delta E_{pi}(R) + \delta E_{ni}(R)] \tag{11}$$

Figure 5. The liquid drop model, E_{LD}, the shell correction, δE, and the total deformation energies, E, for the ^{10}Be accompanied cold fission of ^{252}Cf with ^{146}Ba and ^{96}Sr heavy fragments. The new minimum appears in the shaded area from R_{ov3} to R_t.

which are given by

$$\delta E_{pi} = Cs(Z_i); \quad \delta E_{ni} = Cs(N_i) \tag{12}$$

where

$$s(Z) = F(Z)/[(Z)^{-2/3}] - cZ^{1/3} \tag{13}$$

$$F(n) = \frac{3}{5}\left[\frac{N_i^{5/3} - N_{i-1}^{5/3}}{N_i - N_{i-1}}(n - N_{i-1}) - n^{5/3} + N_{i-1}^{5/3}\right] \tag{14}$$

in which $n \in (N_{i-1}, N_i)$ is either a current Z or N number and N_{i-1}, N_i are the closest magic numbers. The constants $c = 0.2$, $C = 6.2$ MeV were determined by fit to the experimental masses and deformations. The variation with R is calculated [18] as

$$\delta E(R) = \frac{C}{2}\left\{\sum_i [s(N_i) + s(Z_i)]\frac{L_i(R)}{R_i}\right\} \tag{15}$$

where $L_i(R)$ are the lengths of the fragments along the axis of symmetry, at a given separation distance R. During the deformation, the variation of separation distance between centers, R, induces the variation of the geometrical quantities and of the corresponding nucleon numbers. Each time a proton or neutron number reaches a magic value, the correction energy passes through a minimum, and it has a maximum at midshell (see Fig. 5 and Fig. 6). The first narrow minimum appearing in the shell correction energy δE in Fig. 5, at $R = R_{min1b} \simeq 2.6$ fm, is the result of almost simultaneously reaching the
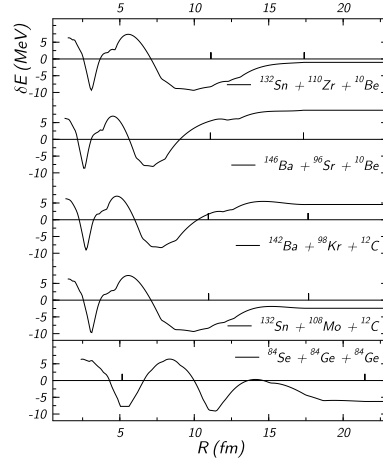
Figure 6. The shell correction energy variation with the separation distance for two examples of ^{10}Be-, two of ^{12}C accompanied cold fission, compared to the "true" ternary fission (in nearly three identical fragments) of ^{252}Cf. The three partners are given. The two vertical bars on each plot show the positions of R_{ov3} and of R_t.

magic numbers $Z_1 = 20$, $N_1 = 28$, and $Z_2 = 82$, $N_2 = 126$. The second, more shallower one around $R = R_{min2b} \simeq 7.2$ fm corresponds to a larger range of R-values for which $Z_1 = 50$, $N_1 = 82$, $Z_2 = 50$, $N_2 = 82$ are not obtained in the same time. In the region of the new minimum, $R = R_{min-t}$, for light-particle accompanied fission, the variation of the shell correction energy is very small, hence it has no major consequence. One can say that the quasimolecular minimum is related to the collective properties (liquid-drop like behavior). On the other side, for "true" ternary process (see the bottom part of Fig. 6) both minima appear in this range of values, but no such LDM effect was found there. In order to compute the half-life of the quasi-molecular state, we have first to search for the minimum E_{min} in the quasimolecular well, from R_{ov3} to R_t, and then to add a zero point vibration energy, E_v: $E_{qs} = E_{min} + E_v$.

The half-life, T, is expressed in terms of the barrier penetrability, P, which is calculated from an action integral, K, given by the quasi-classical WKB approximation

$$T = \frac{h \ln 2}{2 E_v P}; \quad P = exp(-K) \tag{16}$$

Table 1. Calculated half-lives of some quasi-molecular states formed during the ternary fission of ^{252}Cf.

Particle	Fragments		Q_{exp} (MeV)	K	$\log T(s)$
^{10}Be	^{132}Sn	^{110}Ru	220.183	19.96	-11.17
	^{138}Te	^{104}Mo	209.682	25.23	-8.89
	^{138}Xe	^{104}Zr	209.882	26.04	-8.54
	^{146}Ba	^{96}Sr	201.486	22.98	-9.86
^{12}C	^{147}La	^{93}Br	196.268	39.80	-2.56
	^{142}Ba	^{98}Kr	199.896	42.71	-1.30
	^{140}Te	^{100}Zr	209.728	38.21	-3.25
	^{132}Sn	^{108}Mo	223.839	31.46	-6.18

where h is the Planck constant, and

$$K = \frac{2}{\hbar} \int_{R_a}^{R_b} \sqrt{2\mu[E(R) - E_{qs}]} \, dR \qquad (17)$$

in which R_a, R_b are the turning points, defined by $E(R_a) = E(R_b) = E_{qs}$ and the nuclear inertia is roughly approximated by the reduced mass $\mu = m[(A_1 A_2 + A_3 A)/(A_1 + A_2)]$, where m is the nucleon mass, $\log[(h\ln 2)/2] = -20.8436$, $\log e = 0.43429$ and $\sqrt{8m/\hbar^2} = 0.4392$ MeV$^{-1/2}\times$fm^{-1}.

The results of our estimations for the half-lives of some quasimolecular states formed in the ^{10}Be- and ^{12}C accompanied fission of ^{252}Cf are given in Table 1. They are of the order of 1 ns and 1 ms, respectively, if we ignore the results for a division with heavy fragment ^{132}Sn, which was not measured due to very high first excited state. Consequently the new minimum we found can qualitatively explain the quasimolecular nature of the narrow line of the ^{10}Be γ-rays.

It is interesting to note that the trend toward a split into two, three, or four nuclei (the lighter ones formed in a long neck between the heavier fragments) has been theoretically demonstrated by Hill, [19] who investigated the classical dynamics of an incompressible, irrotational, uniformly charged liquid drop. No mass asymmetry was evidenced since any shell effect was ignored.

In conclusion, we should stress that a quasimolecular stage of a light-

particle accompanied fission process, for a limited range of sizes of the three partners, can be qualitatively explained within the liquid drop model.

Acknowledgments

References

1. L. W. Alvarez, as reported by G. Farwell, E. Segrè, and C. Wiegand, *Phys. Rev.* **71**, 327 (1947). T. San-Tsiang *et al.*, *C. R. Acad. Sci. Paris* **223**, 986 (1946).
2. M. Mutterer and J.P. Theobald, in *Nuclear Decay Modes*, ed. D.N. Poenaru (IOP Pub., Bristol, 1996), p. 487.
3. N. Bohr and J. Wheeler, *Phys. Rev.* **55**, 426 (1939).
4. V.M. Strutinsky, *Nucl. Phys.* A **95**, 420 (1966).
5. W.D. Myers and W.J. Swiatecki, *Nucl. Phys.* A **81**, 1 (1966).
6. D.N. Poenaru and W. Greiner, in *Nuclear Decay Modes*, (IOP Publishing, Bristol, 1996), p. 275.
7. A. Săndulescu, D.N. Poenaru and W. Greiner, *Sov. J. Part. Nucl.* **11**, 528 (1980).
8. C. Signarbieux *et al.*, *J. Phys. Lett. (Paris)* **42**, L437 (1981).
9. E.K. Hulet *et al.*, *Phys. Rev. Lett.* **56**, 313 (1986).
10. A.V. Ramayya *et al.*, *Phys. Rev.* C **57**, 2370 (1998).
11. A.V. Ramayya *et al.*, *Phys. Rev. Lett.* **81**, 947 (1998).
12. J.H. Hamilton *et al.*, *Prog. Part. Nucl. Phys.* **35**, 635 (1995). G.M. Ter-Akopian *et al.*, *Phys. Rev. Lett.* **77**, 32 (1996).
13. P. Singer *et al.*, in *Dynamical Aspects of Nuclear Fission*, Proc. 3rd Int. Conf., Častá-Papiernička, Slovakia, 1996 (JINR, Dubna, 1996), p. 262.
14. D.A. Bromley *et al.*, *Phys. Rev. Lett.* **4**, 365 (1960).
15. W. Greiner, J.Y. Park, W. Scheid, *Nuclear Molecules* (World Sci., Singapore, 1995).
16. D.N. Poenaru *et al.*, *Phys. Rev.* C **59**, 3457 (1999).
17. D.N. Poenaru and M. Ivaşcu, *Comput. Phys. Commun.* **16**, 85 (1978).
18. H. Schultheis and R. Schultheis, *Phys. Lett.* B **37**, 467 (1971).
19. D.L. Hill in *Proc. of the 2nd U N Int. Conf. on the Peaceful Uses of Atomic Energy* (United Nations, Geneva, 1958), p. 244.